

*Short Communication*

# Calcined Clay and Limestone as Partial Replacements of Portland Cement: Electrochemical Corrosion Behavior of Low Carbon Steel Rebar as Concrete Reinforcement in Corrosive Environment

Fengren Guo\*

Fujian Polytechnic of Information Technology, Department of Architectural Engineering, Fujian Fuzhou, 350003, China

\*E-mail: [gfr219@126.com](mailto:gfr219@126.com)

*Received:* 1 August 2020 / *Accepted:* 22 September 2020 / *Published:* 31 October 2020

---

Recent studies indicate that corrosion resistance of reinforced concrete could be improved by enhancing the concrete structure, particularly Portland cement (PC) replacement by mineral compounds. In this study, the effect of calcined clay (CC) and limestone (LS) as partial replacement of PC on corrosion resistance of HRB500 carbon steel reinforced concrete in 3.5% NaCl solution were considered. After curing for one day, the PC replaced with both CC and LS admixtures revealed the strength of 28 MPa while the mixture with only limestone showed a compressive strength of 21 MPa. The lower strength in blended concretes than the PC mixture can be attributed to the effect of cement dilution. Water absorption results indicate that transport of chloride ions, liquid and moisture is greatly reduced, mostly due to the pore structure refinement of the concrete sample with LS and CC admixtures. The polarization results reveal that the concrete specimens containing CC and LS admixtures had a lower corrosion value on the surface of carbon steel compared to the other specimens. The EIS findings exhibited that the double-layer capacitance value reduced for the concrete sample including both LS and CC admixtures, showing the passive layer thickness was enhanced and resulting in an improved protective capacity.

---

**Keywords:** Calcined clay and limestone admixtures; Electrochemical corrosion behavior; carbon steel rebar; Portland cement

## 1. INTRODUCTION

Carbon steel in reinforced concrete offers the essential tensile properties into concrete structure. Corrosion in steel reinforced concrete has received much attention due to its importance in durability of the structures [1, 2]. Corrosion is the slow degradation of materials because of chemical reaction

with the corrosive environment, which contains electrochemical reaction that depend on the transport of electrons to the adjacent material [3-5]. Concrete permeability is a negative feature of concrete durability because it easily transports water or other liquids over the concrete and then carries corrosive materials [6, 7]. Researchers have done a lot of research to develop the durability of the concrete structures. Recently, there are many approaches to extend lifespan of the reinforced structures immersed to the corrosive environments, containing the coated materials on steel reinforcement, corrosion inhibitors and non-ferrous reinforcement [8-10]. A partial replacement of ordinary Portland cement (OPC) through mineral admixtures can be another viable and ecological choice for corrosion resistance [11]. The mineral admixtures reduces the porosity and permeability of concrete due to the creation of cementitious mixtures through a pozzolanic reaction with the calcium hydroxide ( $\text{Ca}(\text{OH})_2$ ) from the hydration of cement [12-14].

Different types of mineral materials, such as metallic based furnace slag, marble waste dust, limestone, silica fume, fly ash and tire rubbers have been commonly used into the concrete structures [15]. Previous research has shown that these compounds can improve the properties of concrete structures, specifically its compressive strength, workability and durability in the concrete structures.

Limestone (LS) admixture is commonly used as mineral additive in self-compacting concrete. Many investigations have been done to develop concrete replaced by different kinds of admixtures such as limestone which caused the development of its chemical resistance and mechanical properties [16-18]. A partial replacement of OPC by calcined clay (CC) makes a substantial modification in chemical and physical properties which makes them suitable for the concrete construction [19, 20].

Since the simultaneous effects of CC and LS on corrosion resistance of steel reinforced concretes have not been previously reported. In this work, the electrochemical corrosion behavior of HRB500 carbon steel rebar reinforced in concrete containing CC and LS were considered. Polarization analysis, electrochemical impedance spectroscopy (EIS) measurement, and open-circuit potential (OCP) characterization were used to investigate the corrosion resistance of carbon steel rebar.

## 2. MATERIALS AND METHODS

In order to study the electrochemical corrosion of reinforced concrete, HRB500 carbon steel was used as a rebar. The chemical composition of HRB500 carbon steel is shown in table 1. The Steel rebars were cleaned and washed with SiC paper and ethanol solution, respectively.

**Table 1.** Chemical composition of the HRB500 carbon steel (wt%).

Element	Content (%)
Fe	Residual
Mn	1.5
P	0.03
Si	0.55
C	0.20
S	0.025

The concrete structures were cast by different content of calcined clay (CC) and limestone (LS) with replacement of Portland cement (PC). The chemical compositions of CC and LS are indicated in Table 2. The PC was blended with sand, gravel, and water (1.5: 3: 1: 0.48) to make concrete samples. The mixed cements were prepared by a high-speed mixer system to achieve a heterogeneous dispersion.

In order to prepare working electrodes, the concrete mixture was poured into the cylindrical mold, while a steel rebar was placed vertically at the center of the cylinder. The carbon steel rebar with 1 cm diameter and the 7 cm length was positioned in the center of the cylinder mold with 4 cm diameter. The reinforced concrete specimens were cast and subsequently the molds were eliminated after 24 h curing time. The concrete mix ratios are revealed in Table 3.

**Table 2.** Chemical compositions of the CC, limestone and PC

Parameters	PC	CC	LS
SiO <sub>2</sub> (%)	19.98	54.74	0.55
Al <sub>2</sub> O <sub>3</sub> (%)	4.74	41.02	0.40
Fe <sub>2</sub> O <sub>3</sub> (%)	3.02	1.21	0.17
CaO (%)	63.53	0.03	53.47
MgO (%)	2.04	0.4	1.02
K <sub>2</sub> O (%)	0.65	2.19	0.03
Na <sub>2</sub> O (%)	0.27	0.06	0.01
SO <sub>3</sub> (%)	2.65	0.03	0.00
LOI (%)	3.12	0.32	43.13

**Table 3.** Details of the concrete mixtures

Samples	PC	10L	10L10C
PC (kg/m <sup>3</sup> )	500	450	400
LS (kg/m <sup>3</sup> )	0.0	50	50
CC (kg/m <sup>3</sup> )	0.0	0.0	50
Sand (kg/m <sup>3</sup> )	1000	1000	1000
Gravel (kg/m <sup>3</sup> )	333	333	333
Water (kg/m <sup>3</sup> )	240	240	240

The compressive strengths of the samples were considered according to ASTM C39-81. The EIS experiments were done by a model EA-201 Electrolyte Analyzer and a typical personal computer which was used for electrochemical assessment. A three-electrode cell was used during the EIS experiments, with carbon steel reinforced concrete, a platinum electrode and a saturated calomel electrode as a working, counter and reference electrodes, respectively. All analyses were done after exposed to 3.5wt% NaCl solution. The EIS measurements were performed at the frequency range of 0.1 MHz and 0.01 Hz. The half-cell potential measurements are applied to estimate the corrosion

potential of each sample according to ASTM C876-15 standards. The potentiodynamic polarization test was conducted in the potential ranges of -0.8 to -0.0 V at scanning rate of 1 mV/s. The scanning electron microscope (SEM) was used to consider the surface morphologies of the samples. The polarization analysis was done from 250 mV at a scan rate of 1 mV/s.

### 3. RESULTS AND DISCUSSION

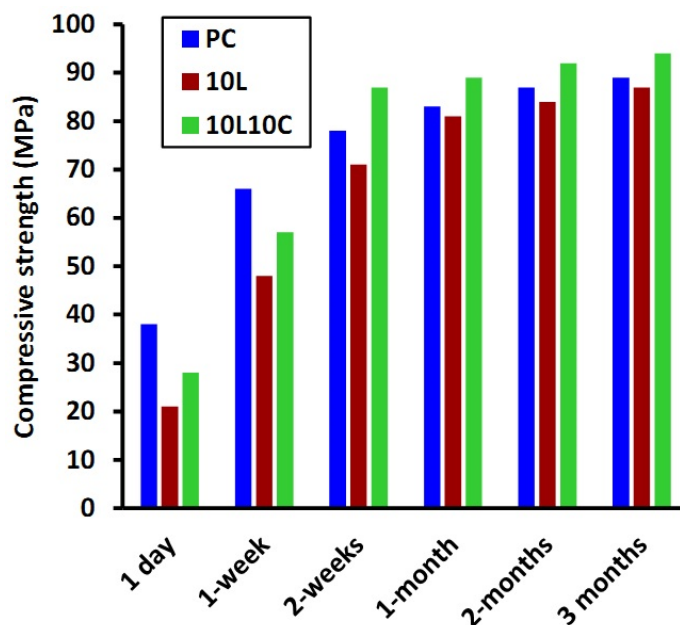


**Figure 1.** The compressive strength of concrete samples with different admixtures at room temperature

The compressive strength for each admixture is shown in Figure 1. All the mixtures indicated an increase in compressive strength from one day to three months. After curing for one day, PC mix exhibited an average strength of 38 MPa. The PC replaced with both CC and LS admixtures revealed the strength of 28 MPa while the mixture with only limestone showed a compressive strength of 21 MPa. The lower strength in blended concretes than the PC mixture can be attributed to the effect of cement dilution. Furthermore, the comparable strength between mixed cement and filler mixtures indicates that the pozzolanic reaction on the first day is remarkable to cause strength enhancement. After curing for one week, the PC samples still indicate the highest compressive strength of 66 MPa. The 10L sample shows compressive strength of 48 MPa. As shown in figure 1, the mix 10L10C exhibited a higher rate of strength enhancement (57 MPa) than the 10L sample. This tendency is even more pronounced at two weeks of age, with a 10L10C sample indicating the highest strength of 87 MPa, while the PC mixture shows 78 MPa. It can be related to the pozzolanic reaction at the CC and its synergizing action by LS. Mixture 10L indicates a strength of 71 MPa at two weeks of age, close to that of a PC sample. The increase of strength rate from two weeks to three months is almost the same for all mixtures, indicating the LS and CC reaction may be completed in the two weeks because of the small amount of water for the chemical reactions in the mixture.

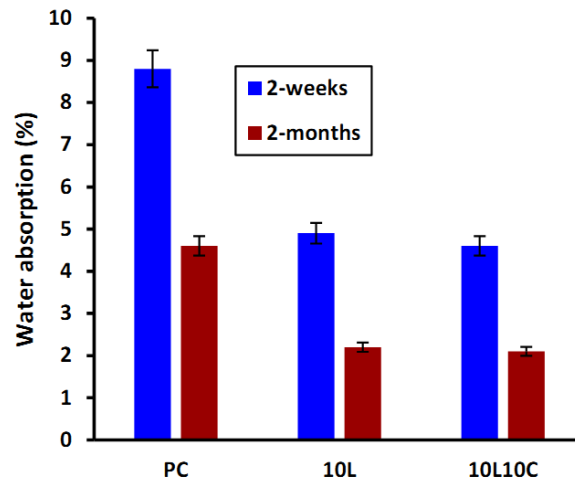


**Figure 2.** Water absorption of concrete samples with and without LS and CC admixtures at two weeks and two months

Figure 2 shows the influence of blended LS and CC on the initial water absorption of concrete samples at two weeks and two months. The initial water absorption reduces with longer age for all mixtures because of the microstructural evolution related to the continuous cement hydration. At two weeks, PC mixture has the highest water absorption. The CC and LS replacement can significantly decrease the absorption by about 55%. Similar decreasing trend in absorption can be observed in three months. Absorption is a main index to consider the concrete resistance to moisture due to capillary adsorption. The absorption of cement composites is principally controlled by the connectivity, pore size and total porosity which provides the moisture pathways. The incorporation of mixed LS and CC can make more dense interfacial transition zones between cement matrix and aggregates and also refine the pore structures of the bulk paste. The achieved results are in accordance with previous studies [21].

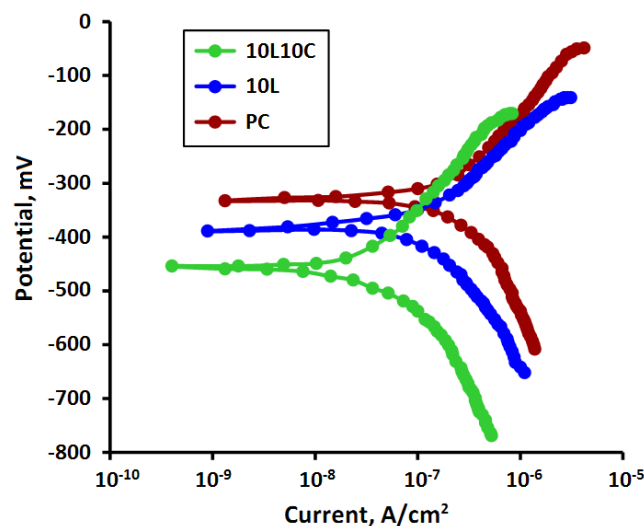


**Figure 3.** Polarization curves of HRB500 carbon steel reinforced concrete with different admixtures exposed to 3.5 wt% NaCl after two months exposure time at scanning rate of 1 mV/s.

Figure 3 reveals polarization curves of HRB500 carbon steel reinforced concrete with different admixtures exposed to 3.5 wt% NaCl after two months immersion time. The corrosion parameters achieved from polarization plots are shown in Table 4. As indicated, the 10L10C concrete containing both LS and CC admixtures was shown to have a higher value of corrosion potential. Moreover, it was observed that the 10L10C specimen had a smaller value of current density than the PC and 10L samples. The superior performance of 10L10C sample was caused by the influence of LS and CC admixtures which enhanced the hydration reaction due to the high specific area and reactivity of their structures. It can produce a denser concrete and reduce the permeability of mortar and decrease the current flow [22, 23]. Furthermore, the lower current density at the 10L10C sample can be related to the variation in the thickness or the structure of the passive film on the surface of carbon steel rebars [24]. Additionally, the concrete specimen containing both LS and CC admixtures indicated a lower corrosion rate ( $0.82 \times 10^{-3}$  MMPY) than the PC concrete. The results indicate that the 10L10C sample had a lower corrosion value on the surface of carbon steel compared to the other specimens.

**Table 4.** The achieved data for corrosion parameters from polarization plots of steel rebar embedded in various concrete specimens

Sample	Corrosion current density ( $\mu\text{A}/\text{cm}^2$ )	Corrosion potential (mV)	Corrosion rate (MMPY) $\times 10^{-3}$
PC	0.42	-334	2.8
10L	0.08	-388	1.7
10L10C	0.05	-456	0.82

Table 5 shows the corrosion parameter comparison of different admixtures as mentioned in the literature. The results indicated that the 10L10C sample for corrosion potential and corrosion current density of carbon steel were comparable with other admixtures obtained from the literature.

**Table 5.** The corrosion parameter comparison of different admixtures as mentioned in the literature

Admixture	Environment	Corrosion current density ( $\mu\text{A}/\text{cm}^2$ )	Corrosion potential (mV)	Ref.
Calcined Clay and Limestone	3.5% NaCl	0.05	-456	This work
Silica Fume and Fly Ash	3.5% NaCl	0.06	-238	[25]
Marble dust and silica fume	5% NaCl	0.032	-247	[26]
Fly ash	3.5% NaCl	0.46	-520	[27]
Bagasse ash	3.5% NaCl	0.093	-164	[28]

The EIS analysis of HRB500 carbon steel rebars were investigated after two months exposure to a marine environment. The Nyquist plots of the reinforced concrete samples with different

admixture contents are revealed in Fig. 4. As shown, all mixes indicate two capacitive properties. The low-frequency loop is related to the steel surface. The high-frequency loop from the Nyquist plot is associated with the concrete sample that covers the steel reinforced concrete. Hence, an equivalent circuit model was used in this work which is revealed in Fig. 5. The equivalent circuit includes a parallel resistance ( $R_c$ ) and capacitance ( $Q_c$ ) for covered concrete at high-frequencies in series with parallel charge-transfer resistance ( $R_{ct}$ ) and double-layer capacitance ( $Q_{dl}$ ) of the carbon steel surface in low-frequencies [29]. Given that the steel surface did not perform as a total capacitor in the electrochemical process, thus a constant-phase element was applied to model the double-layer.  $R_s$  indicates solution resistance. The  $R_s$  value was related to the electrolyte solution resistivity, which was insignificant compared with the resistance of other elements [30].

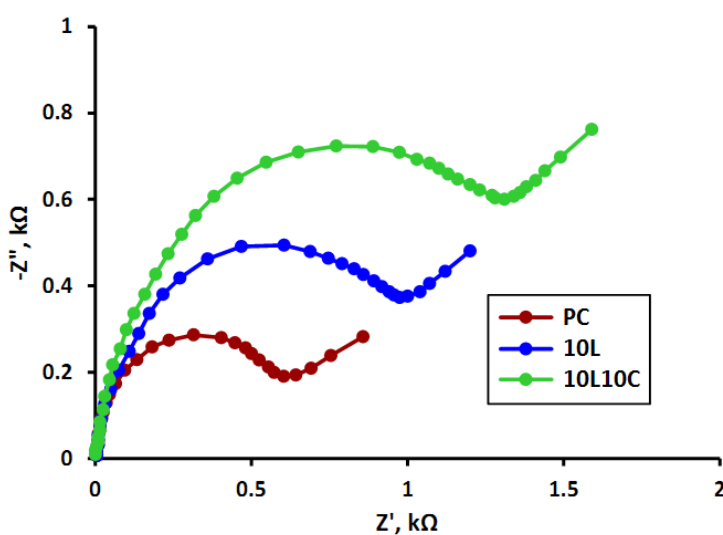


**Figure 4.** EIS plots of reinforced concrete specimens with different admixture contents after two months exposure to 3.5% NaCl solution in the frequency range of 100 kHz to 0.1 mHz at room temperature.

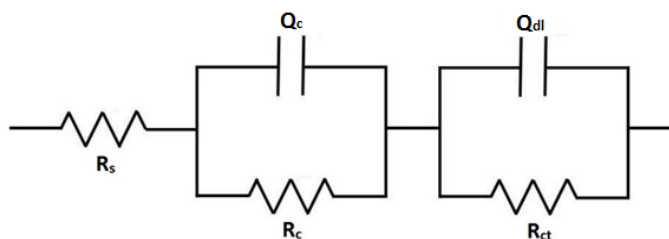


**Figure 5.** The used equivalent circuit model

**Table 6.** EIS parameters derived from Fig. 4 for carbon steel rebar in various concrete specimens after two months immersed in 3.5% NaCl solution

Sample	$R_s$ ( $\Omega \text{ cm}^2$ )	$R_c$ ( $\text{k}\Omega \text{ cm}^2$ )	$Q_c$ ( $\mu\text{F cm}^{-2}$ )	$R_{ct}$ ( $\text{k}\Omega \text{ cm}^2$ )	$Q_{dl}$ ( $\mu\text{F cm}^{-2}$ )	$R_p$ ( $\text{k}\Omega \text{ cm}^2$ )
PC	51.4	0.38	3.3	0.76	4.8	1.14
10L	42.2	0.66	1.9	1.26	2.7	1.92
10L10C	53.6	0.97	1.2	1.78	1.8	2.75

As shown in table 6, the  $R_{ct}$  value of specimens increases with addition of the admixtures into the PC structure. Furthermore, the 10L10C sample shows higher value of the  $R_{ct}$  than the others, which shows that simultaneous use of LS and CC admixtures as partial replacement into the PC can improve the corrosion behavior of carbon steel rebars. It can be associated with the enhancement of the concrete microstructure due to the filler action and improvement of bonding capability in the LS and CC particles which can decrease the air content, porosity and pore diameters, resulting in enhancing the internal surface area of the cement-matrix. Therefore, it can cause a reduction in permeability of concrete-matrix. Polarization resistance can be used to study the charge transfer rate in the interface film [31]. As shown, the values of  $R_p$  increase with addition of the admixtures into the PC structure, which reduces the corrosion probability. Thus, using mineral admixtures may enhance the carbon steel rebar surface and help long-term corrosion resistance which is in agreement with previous studies [32, 33].

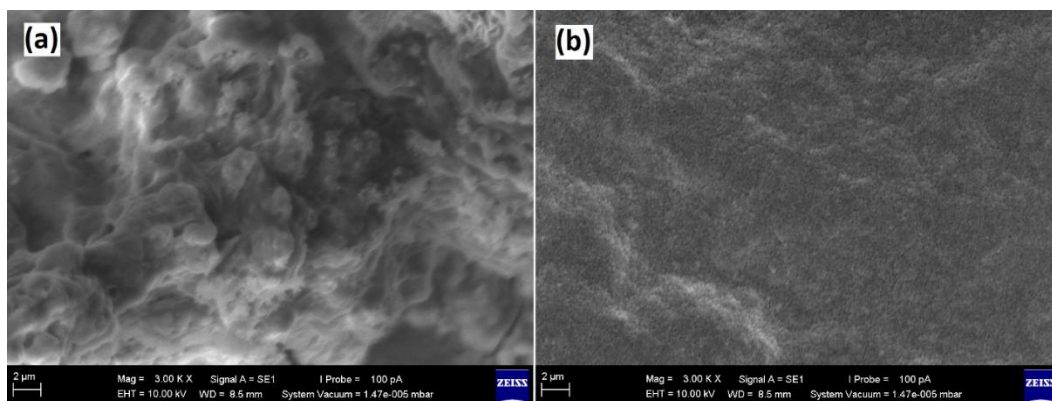
**Figure 6.** FESEM images of HRB500 carbon steel reinforced concrete with different admixtures (a) PC and (b) LS and CC after exposed to 3.5 wt% NaCl solution after two months exposure time at room temperature

Figure 6 reveals the surface morphology of HRB500 carbon steel reinforced concrete with different admixtures exposed to 3.5% NaCl solution after two months. The separation and irregularity structures were enhanced by addition of LS and CC admixtures. Figure 6b indicates that the rebar surface embedded in 10L10C concrete is more uniform compared to the PC specimen which are basically in agreement with electrochemical results. The calcined clay contains high concentrations of

Al<sub>2</sub>O<sub>3</sub> and SiO<sub>2</sub>, which reduce the heat of hydration affected by the water-cement reaction. On the other hand, the limestone as a filler decreases concrete permeability and enhances its durability and prevents the corrosive ions from attaining the surface of carbon steel rebars.

#### 4. CONCLUSIONS

Newly, mineral admixtures have been used in concrete structures as partial replacement of cement for economic and environmental reasons. In this work, an electrochemical study on corrosion behavior of HRB500 carbon steel rebar in concrete samples with LS and CC admixtures were done. In order to investigate corrosion resistance of the carbon steel reinforced concretes, potentiodynamic polarization and EIS analysis were performed after two months exposure time. Water absorption results indicate that transport of chloride ions, liquid and moisture is greatly reduced, mostly due to the pore structure refinement of the concrete sample with LS and CC admixtures. The polarization results reveal that the concrete specimens containing CC and LS admixtures had a lower corrosion value on the surface of carbon steel compared to the other specimens. The EIS findings exhibited that the double-layer capacitance value reduced for the concrete sample including both LS and CC admixtures, showing the passive layer thickness was enhanced and resulting in an improved protective capacity.

#### References

1. V. Volpi-León, L. López-Léon, J. Hernández-Ávila, M. Baltazar-Zamora, F. Olguín-Coca and A. López-León, *International Journal of Electrochemical Science*, 12 (2017) 22.
2. S. Kakooei, H.M. Akil, M. Jamshidi and J. Rouhi, *Construction and Building Materials*, 27 (2012) 73.
3. X. Zheng, H. Castaneda, H. Gao and A. Srivastava, *Corrosion Science*, 153 (2019) 53.
4. S. Zhang, H. Li, Z. Jiang, B. Zhang, Z. Li, J. Wu, H. Feng, H. Zhu and F. Duan, *Corrosion Science*, 163 (2020) 108295.
5. R. Dalvand, S. Mahmud, J. Rouhi and C.R. Ooi, *Materials Letters*, 146 (2015) 65.
6. U.M. Angst, M.R. Geiker, M.C. Alonso, R. Polder, O.B. Isgor, B. Elsener, H. Wong, A. Michel, K. Hornbostel and C. Gehlen, *Materials and Structures*, 52 (2019) 88.
7. X. Wang, M. Sun and S. Guo, *Construction and Building Materials*, 220 (2019) 607.
8. G. Duffó, S. Farina and F.S. Rodríguez, *Construction and Building Materials*, 210 (2019) 548.
9. J. Rouhi, S. Mahmud, S.D. Hutagalung and N. Naderi, *Electronics letters*, 48 (2012) 712.
10. S. Kakooei, H.M. Akil, A. Dolati and J. Rouhi, *Construction and Building Materials*, 35 (2012) 564.
11. K. Kupwade-Patil, C. De Wolf, S. Chin, J. Ochsendorf, A.E. Hajjah, A. Al-Mumin and O. Büyükoztürk, *Journal of cleaner production*, 177 (2018) 547.
12. G. Girskas and G. Skripkiūnas, *Construction and Building Materials*, 142 (2017) 117.
13. C. Medina, I.F. Saez del Bosque, E. Asensio, M. Frías and M.I. Sánchez de Rojas, *Journal of the American Ceramic Society*, 99 (2016) 340.
14. J. Rouhi, S. Mahmud, S.D. Hutagalung, N. Naderi, S. Kakooei and M.J. Abdullah, *Semiconductor Science and Technology*, 27 (2012) 065001.
15. V. Nežerka, P. Bílý, V. Hrbek and J. Fládr, *Cement and Concrete Composites*, 103 (2019) 252.
16. G. Sua-iam, P. Sokrai and N. Makul, *Construction and Building Materials*, 125 (2016) 1028.

17. H. Yang, C. Lu and G. Mei, *Journal of Materials in Civil Engineering*, 30 (2018) 04017282.
18. J. Rouhi, S. Mahmud, S.D. Hutagalung and S. Kakooei, *Journal of Micro/Nanolithography, MEMS, and MOEMS*, 10 (2011) 043002.
19. K. Scrivener, F. Martirena, S. Bishnoi and S. Maity, *Cement and Concrete Research*, 114 (2018) 49.
20. S. Ferreiro, M. Canut, J. Lund and D. Herfort, *Applied Clay Science*, 169 (2019) 81.
21. Y. Dhandapani, T. Sakthivel, M. Santhanam, R. Gettu and R.G. Pillai, *Cement and Concrete Research*, 107 (2018) 136.
22. R. Yu, P. Spiesz and H. Brouwers, *Construction and Building Materials*, 65 (2014) 140.
23. R. Dalvand, S. Mahmud and J. Rouhi, *Materials Letters*, 160 (2015) 444.
24. Y. Chou, J. Yeh and H. Shih, *Corrosion Science*, 52 (2010) 2571.
25. M.A. Baltazar-Zamora, D. M Bastidas, G. Santiago-Hurtado, J.M. Mendoza-Rangel, C. Gaona-Tiburcio, J.M. Bastidas and F. Almeraya-Calderón, *Materials*, 12 (2019) 4007.
26. W.Z. Shengpin Liu, *International Journal of Electrochemical Science*, 15 (2020) 3825.
27. Y.-S. Choi, J.-G. Kim and K.-M. Lee, *Corrosion Science*, 48 (2006) 1733.
28. Q. Zhang, H. Li, H. Feng and T. Jiang, *International Journal of Electrochemical Science*, 15 (2020) 6135.
29. J.Z. Du Fengyin, Z. Tiejun and D. Xueyan, *International Journal of Electrochemical Science*, 13 (2018) 7076.
30. N. Naderi, M. Hashim and J. Rouhi, *International Journal of Electrochemical Science*, 7 (2012) 8481.
31. T. Yang, J. Liu, Y. Yu, Y.-L. Lee, H. Finklea, X. Liu, H.W. Abernathy and G.A. Hackett, *Physical Chemistry Chemical Physics*, 19 (2017) 30464.
32. J. Wei, S. Ma and G.T. D'Shawn, *Corrosion Science*, 106 (2016) 1.
33. D. Wang, X. Zhou, B. Fu and L. Zhang, *Construction and Building Materials*, 169 (2018) 740.